Acta Crystallographica Section D
Biological Crystallography
ISSN 0907-4449

Structure of the 'open' form of *Aspergillus nidulans* 3-dehydroquinate synthase at 1.7 Å resolution from crystals grown following enzyme turnover

C. E. Nichols,[a] A. R. Hawkins[b] and D. K. Stammers[a]*

[a]Division of Structural Biology, The Wellcome Trust Centre for Human Genetics, University of Oxford, Roosevelt Drive, Oxford OX3 7BN, England, and [b]School of Cell and Molecular Biosciences, Medical School, Catherine Cookson Building, Framlington Place, University of Newcastle-upon-Tyne NE2 4HH, England

Correspondence e-mail: daves@strubi.ox.ac.uk

Received 15 December 2003
Accepted 1 March 2004

PDB Reference: 3-dehydroquinate synthase, 1sg6, r1sg6sf.

Crystallization of *Aspergillus nidulans* 3-dehydroquinate synthase (DHQS), following turnover of the enzyme by addition of the substrate DAHP, gave a new crystal form (form *J*). Although the crystals have dimensions of only 50 × 20 × 5 µm, they are well ordered, diffracting to 1.7 Å. The space group is $C222_1$, with unit-cell parameters a = 90.0, b = 103.7, c = 177.4 Å. Structure determination and refinement to R = 0.19 ($R_{\rm free}$ = 0.25) shows the DHQS is in the 'open' form with the substrate site unoccupied but with some loop regions perturbed. Previous crystals of open-form DHQS only diffracted to 2.5 Å resolution. The use of enzyme turnover may be applicable in other systems in attempts to improve crystal quality.

1. Introduction

The enzyme dehydroquinate synthase (DHQS) catalyses the conversion of 3-deoxy-D-*arabino*-heptulosonate-7-phosphate (DAHP) to dehydroquinate (DHQ), an intermediate in the biosynthesis of shikimate. The shikimate pathway is present in bacteria and microbial eukaryotes, but is absent in higher eukaryotes (Bentley, 1990). Pathogenic bacteria mutants in this pathway are attenuated for virulence (Gunel-Ozcan *et al.*, 1997). Enzymes such as DHQS thus represent attractive targets for the development of novel antimicrobial drugs.

DHQS has been thoroughly characterized biochemically (Bender *et al.*, 1989; Moore *et al.*, 1994; Knowles, 1989; Widlanski *et al.*, 1989). More recently, X-ray crystal structures of *Aspergillus nidulans* DHQS (*An*DHQS) have led to proposals for the mechanisms of catalysis (Carpenter *et al.*, 1998) and domain closure (Nichols *et al.*, 2003).

We previously reported the identification of nine different crystal forms of *An*DHQS (forms *A*–*I*; Nichols *et al.*, 2001). Structure determination indicated that in the absence of the substrate analogue carbaphosphonate (CBP), DHQS was in an open form with a domain rotation of ∼12° (Brown *et al.*, 2003; Nichols *et al.*, 2003) compared with the closed ternary complex (Carpenter *et al.*, 1998). The mechanisms involved in the domain closure are complex: there are changes in three proximal elements that have substrate-contacting residues in the closed form (PE1–PE3) which propagate to five distal elements having no direct contact with the substrate (DE1–DE5). These two sets of changes then act concertedly to cause the large-scale closure of the hinge, leading to the exclusion of bulk solvent and the formation of a tightly defined active-site pocket. The maximum resolution of the earlier crystals of the *An*DHQS open form was ∼2.5 Å, thus limiting the accuracy of the final models. The availability of a higher resolution *An*DHQS open structure will benefit both the design of novel inhibitors as well as detailed analysis of domain movements of the protein. The current work describes the generation of a new crystal form (form *J*) of the open conformation of *An*DHQS diffracting to 1.7 Å resolution, which grew after the addition of an excess of substrate to allow enzyme turnover. Determination of the structure of *An*DHQS in this new crystal form, refinement to 1.7 Å and comparison with the earlier open-form structures are described.

2. Materials and methods

The cloning, expression and isolation of *An*DHQS took place as described previously (Moore *et al.*, 1994; van den Hombergh *et al.*, 1992). For crystallization, aliquots of purified protein were concentrated and buffer-exchanged into 10 m*M* Tris pH 7.4, 40 m*M* KCl using Vivascience Vivaspin 2 centrifugal concentrators with polyethersulfone membranes. Pooled concentrates were filtered through Amersham NAP 25 columns, re-concentrated to 30 mg ml^{-1} and pre-incubated at 277 K with 1 m*M* $ZnCl_2$ for 20 min; 50 m*M* DAHP was then added. Hampton Research sparse-matrix and grid screens were then set up (*i.e.* Crystal Screen I, Crystal Screen II, Crystal Screen Cryo, PEG/Ion, Natrix, MembFac, PEG/LiCl Grid, NaCl Grid, PEG 6000 Grid and A/S Grid Screens). All crystallizations were carried out at 277 K and set up as sitting-drop vapour-diffusion experiments utilizing microbridges.

Single frames of X-ray data were collected from the crystals that grew from the screens and the unit-cell parameters were characterized. A full X-ray diffraction data set was then collected for the new form *J* turnover-related crystal form. Data collection was carried out at the ESRF on beamline ID-14 EH4 (λ = 0.933 Å) at 100 K, with cryoprotection being provided by the displacement of aqueous media with perfluoroether PFO-X125/03 (supplied by Lancaster). Indexing, integration and merging of data images were carried out with *DENZO* and *SCALEPACK* (Otwinowski & Minor, 1996). Rotation-function and translation searches together with initial rigid-body Patterson correlation refinement were carried out using *CNS* (Brünger *et al.*, 1998). Molecular-replacement solutions were checked by displaying the transformed coordinates in *O* (Jones *et al.*, 1991). Rigid-body, positional and *B*-factor refinement, simulated annealing and initial water picking were carried out in *CNS*. Manual rebuilding, including insertion of ions, ligands and extra water molecules, was carried out with *O*. The final model was overlaid with previously released *An*DHQS structures using *Top3D* (Collaborative Computational Project, Number 4, 1994); the results were compared visually in *VMD* (Humphrey *et al.*, 1996) and final figures prepared using *Corel*11.

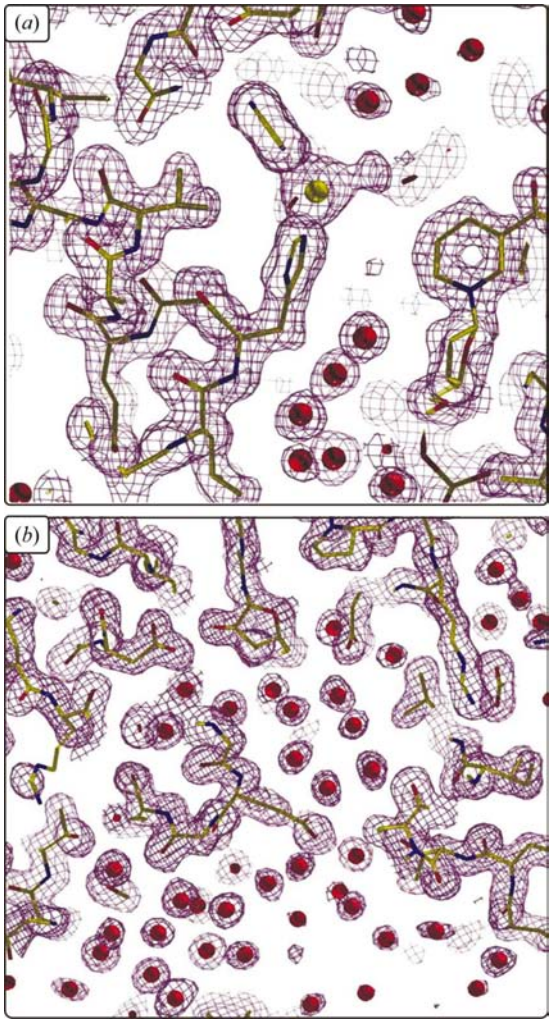

Figure 1
Electron-density map at 1. 7 Å resolution for *An*DHQS showing (*a*) the active-site region and (*b*) the presence of extended hydration shells.

3. Results and discussion

Characterization of crystals deriving from screens set up with *An*DHQS and 50 m*M* DAHP revealed a new crystal form (form *J*) that was obtained under conditions that had not previously been seen to yield crystals with either NAD binary or NAD/CBP ternary setups. Data were therefore collected to determine the structure of the complex involved and compare it with other structures to assess any differences and see if it represented the crystallization of an intermediate stage in the domain-closure cycle. Although the crystals were extremely small (50 × 20 × 5 µm), they proved to be very well ordered, diffracting to 1.7 Å resolution.

Autoindexing with *DENZO* indicated *C*-centred orthorhombic symmetry and analysis of systematic absences then allowed the final assignment of space group as $C222_1$. The *C* chain of PDB model 1nve (NAD binary complex) was used as an initial molecular-replacement search model and the first cross-rotation peak gave a good translation search result with an E2E2 correlation of 0.383, yielding chain *A* of the new form. However, it was not so clear which of the other 22 peaks was the correct solution for the second moiety within the asymmetric unit. The monomeric initial solution was therefore subjected to rigid-body, positional and *B*-factor refinement, which lowered $R_{\rm free}$ from 0.52 to 0.46, and was then used for a second cross-rotation search. The monomeric model was then copied to give chains *A* and *B* overlaid on one another and was used for a second translation search with chain *A* fixed for translation but allowed to move in the final rigid-body stage of the *CNS* translation-search script. The first peak (excluding the origin) of the new cross-rotation search was thus revealed as the correct peak for chain *B*, with the resultant dimer showing an E2E2 correlation of 0.734. Structural refinement from this solution was then trivial, with only minor modifications being required after cyclic application of simulated annealing, positional/*B*-factor refinement and automated water-picking/deleting options. Representative electron density is shown in Figs. 1(*a*) and 1(*b*) and final refinement statistics are given in Table 1.

Table 1
Data-collection and refinement statistics for *An*DHQS crystal form *J*.

Values in parentheses are for the outer shell.

Ligands	NAD, Zn^{2+}
Space group	$C222_1$
Unit-cell parameters (Å)	
a	90.0
b	104.5
c	177.4
Subunits in AU	2
Crystal form	*J*
Resolution range	30.00–1.70 (1.73–1.70)
No. observations	91002 (4311)
Data redundancy	7.2 (4.7)
Completeness (%)	99.6 (94.6)
$R_{\rm merge}$†	0.123 (0.735)
$I/\sigma(I)$	18.89 (2.69)
$R_{\rm work}$‡ (%)	19.5
$R_{\rm free}$‡ (%)	25.0
Residues in§ (%)	
Most favoured regions	92.9
Additionally allowed regions	7.1
Mean *B* factors (Å^2)	
All atoms	24.4
Main chain	18.5
Side chains	25.2
Water	26.6
Ligands	14.1
R.m.s.d. bond lengths (Å)	0.005
R.m.s.d. bond angles (°)	1.19
PDB code	1sg6

† $R_{\rm merge} = \sum I_{\rm obs} - \langle I\rangle / \sum \langle I\rangle$. ‡ $R = \sum_{hkl} |F_{\rm o}(hkl) - F_{\rm c}(hkl)| / \sum_{hkl} |F_{\rm o}(hkl)|$. § Ramachandran plot results from *PROCHECK*.

With $d_{\rm min}$ = 1.7 Å, the final structure is of substantially higher resolution than the best extant open form of *An*DHQS (PDB code 1nve; $d_{\rm min}$ = 2.58 Å) and the model contains in excess of 1300 waters, which is between two and four times greater than the number discernible previously. Second-order and even third-order hydration shells can be unambiguously discerned (Fig. 1*b*), which may be because of the greater order of this crystal form but could also be the result of the use of the cryoprotectant perfluoroether, which stabilizes hydration shells more effectively than, for example, glycerol.

Analysis of $2F_{\rm o} - F_{\rm c}$ and $F_{\rm o} - F_{\rm c}$ maps shows no sign of electron density consistent with the presence of either substrate or

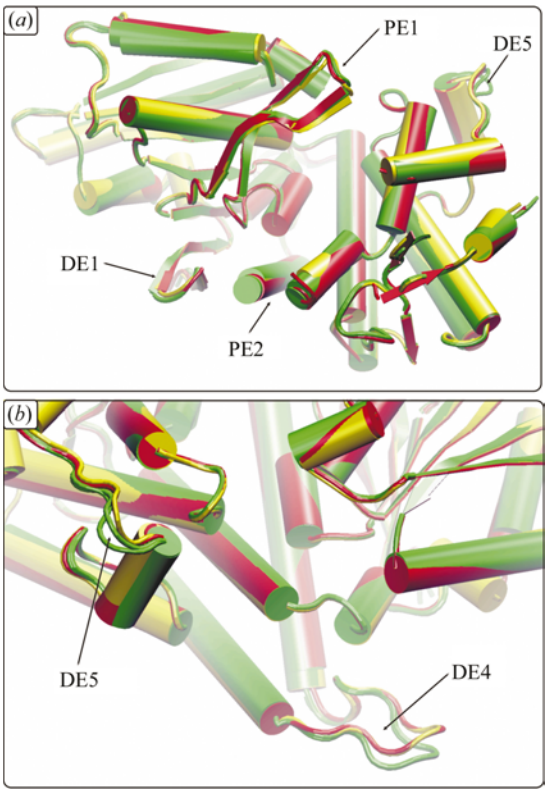

Figure 2
Cartoon-format C^{α}-trace superpositions comparing 'open' *An*DHQSs (NAD complex, crystal form *E*; PDB code 1nve) in green and the structure after turnover (crystal form *J*): chain *A* in yellow, chain *B* in red. (*a*) Full-chain overlap, proximal view. (*b*) Close up of distal hinge-point.

product (Fig. 1*a*), although as expected the tightly bound cofactor NAD is present. Comparison of the refined model with those previously reported for NAD binary and NAD/CBP ternary complexes (PDB models 1nve and 1nr5, respectively) also clearly shows the DHQS is 'open form', with the N- and C-terminal domains counter-rotated by ~12° compared with the 'closed-form' model (Fig. 2*a*). However, whilst the bulk state of the protein is clearly 'open', the *A*-chain PE1 structural element is bent slightly towards the active site (Fig. 2*a*) and in both the *A* and *B* chains structural elements DE1, DE4 and DE5 all show conformations closer to those previously observed with 'closed' rather than 'open-form' structures (Figs. 2*a* and 2*b*). This in turn affects crystal packing, with the semi-disordered DE4 and DE5 regions now making contacts with rigid regions of adjacent moieties in the crystal lattice rather than each other as observed with previous open-form data.

One explanation of the observed conformation of *An*DHQS in crystal form *J* is that as the enzyme relaxes back to the open form after the completion of its reaction cycle, it transiently passes through a conformation that can be trapped to yield this new crystal form. Uncertainty remains as to whether this is truly the final-stage intermediate of domain opening, as the substantial changes in crystal packing may also induce structural changes in the surface contacts relative to their equivalent *in vivo* state. However, it is hoped that the availability of higher resolution open-form *An*DHQS structures will facilitate the future design of inhibitors of this enzyme. In particular, the new structure may aid in the development of compounds which act by stabilizing the open form, an alternative design strategy compared with inhibitors occupying the substrate site. The general utility of enzyme turnover prior to crystallization is difficult to estimate but may be worth using, particularly if other methods fail to give good-quality crystals. We have successfully used this method to crystallize *Varicella zoster* virus thymidine kinase, although in this latter case both products remain bound to the active site following crystallization (Bird *et al.*, 2003).

We are grateful to the staff at the ESRF, Grenoble, France for their assistance with data collection. Financial support for this work was by grants from the BBSRC and Arrow Therapeutics. We thank Dr R. Esnouf for computing support.

References

Bender, S. L., Widlanski, T. & Knowles, J. R. (1989). *Biochemistry*, **28**, 7560–7572.
Bentley, R. (1990). *Crit. Rev. Biochem. Mol. Biol.* **25**, 307–384.
Bird, L. E., Ren, J., Wright, A., Leslie, K. D., Degreve, B., Balzarini, J. & Stammers, D. K. (2003). *J. Biol. Chem.* **278**, 24680–24687.
Brown, K. A., Carpenter, E. P., Watson, K. A., Coggins, J. R., Hawkins, A. R., Koch, M. H. & Svergun, D. I. (2003). *Biochem. Soc. Trans.* **31**, 543–547.
Brünger, A. T., Adams, P. D., Clore, G. M., DeLano, W. L., Gros, P., Grosse-Kunstleve, R. W., Jiang, J.-S., Kuszewski, J., Nilges, M., Pannu, N. S., Read, R. J., Rice, L. M., Simonson, T. & Warren, G. L. (1998). *Acta Cryst.* D**54**, 905–921.
Carpenter, E., Hawkins, A., Frost, J. & Brown, K. (1998). *Nature (London)*, **394**, 299–302.
Collaborative Computational Project, Number 4 (1994). *Acta Cryst.* D**50**, 760–763.
Gunel-Ozcan, A., Brown, K. A., Allen, A. G. & Maskell, D. J. (1997). *Microb. Pathog.* **23**, 311–316.
Hombergh, J. P. M. van den, Moore, J. D., Charles, I. G. & Hawkins, A. R. (1992). *Biochem. J.* **284**, 861–867.
Humphrey, W., Dalke, A. & Schulten, K. (1996). *J. Mol. Graph.* **14**, 27–38.
Jones, T. A., Zou, J. Y., Cowan, S. W. & Kjeldgaard, M. (1991). *Acta Cryst.* A**47**, 110–119.
Knowles, J. R. (1989). *Aldrichim. Acta*, **22**, 59–67.
Moore, J. D., Coggins, J. R., Virden, R. & Hawkins, A. R. (1994). *Biochem. J.* **301**, 297–304.
Nichols, C. E., Ren, J., Lamb, H., Haldane, F., Hawkins, A. R. & Stammers, D. K. (2001). *Acta Cryst.* D**57**, 306–309.
Nichols, C. E., Ren, J., Lamb, H. K., Hawkins, A. R. & Stammers, D. K. (2003). *J. Mol. Biol.* **327**, 129–144.
Otwinowski, Z. & Minor, W. (1996). *Methods Enzymol.* **276**, 307–326.
Widlanski, T., Bender, S. L. & Knowles, J. R. (1989). *Biochemistry*, **28**, 7572–7582.